# Design of flower-shaped high-efficiency compact UWB antenna

*Aicha* Bembarka[1*], *Larbi* Setti[1], *Abdelwahed* Tribak[2], and *Hafid* Tizyi[2]

[1]LSTA, FPL, Abdelmalek Essaadi University, Tetouan, Morocco
[2]Department of Electronics Microwaves and Optics, National Institute of Posts and Telecommunications (INPT), Rabat, Morocco

**Abstract.** The present paper describes a novel planar antenna based on the fractal structure designed for Ultra-Wide Band (UWB) applications. The antenna exceeds the UWB band by covering the frequency range between 7.36 and 19.57 GHz with S11 < -10 dB (the fractional bandwidth is 90.68 %) which involves four applications, the C-band (4-8 GHz), the X-band (8-12 GHz), the Ku-band (12-18 GHz) and the K-band (18-26.5 GHz). The low-cost Rogers RO4003C substrate is employed to print the proposed antenna in a small dimension of 12 x 16.9 x 0.81 mm$^3$. This antenna is invented from the shape of a flower with three elliptical leaves. The antenna simulated radiation efficiency is greater than 97 % with an omnidirectional radiation pattern in the E-plane and a bidirectional radiation pattern in the H-plane, across the entire bandwidth. The maximum realized gain of the proposed antenna is about 5.25 dBi. Therefore, the obtained results demonstrated that the flower-shaped antenna is a good candidate for practical UWB 5G applications.

## 1 Introduction

The new wireless technologies are needing to transmit and receive more data in a faster way. More than that, they need sufficient exploitation of the spectrum, which demands emerging new concepts. The UWB and cognitive radio (CR) paradigms are the best options for overcoming these issues. The CR contributes to better usage of frequency band channels. Furthermore, they aid in the avoidance of signal interference while the frequency channels are in use [1]. Several antennas have been developed for the CR [2–4].

In addition to the CR paradigm, UWB antennas are thought to be viable prospects for future wireless communication systems. They are notable for their resilience to multipath propagation, low power consumption, and ability to transmit a large quantity of data in a short period at local distances ranging from 1 to 10 m. For decades, traditional antennas such as conical, volcano smoke antennas, and coaxial horns were well-known in the design of ultra-wideband antennas, but the advancement of wireless communications necessitated antennas that are compact, inexpensive, and have less complexity [5]. As a result, printed antennas are becoming increasingly popular. As in [6] a UWB Vivaldi antenna is presented that has an overall dimension of 49 x 48 x 0.8 mm$^3$ and covers the frequency from 2.9 to 9 GHz. In order to improve the antenna bandwidth, a combination between Hemi cylinder slots and directors is used. Moreover, planar monopole antennas based on Metamaterial, Octagonal-shaped, and Circular-shaped radiated elements have been reported in [7–10] for UWB applications. The antenna in [8] has a wideband covering the range 3.1-10.6 GHz, has a good gain that varies from -2 to 6 dBi, and is characterized by an efficiency greater than 70 %. In [9] the gain of the antenna is of 5.8 dBi when it resonates between 3.1 and 12 GHz. Authors in [10] proposed an antenna that has a 183.91 % of the fractional bandwidth and has a high efficiency that goes between 83 and 95 %, the antenna gain is between 2.58 and 5.05 dBi. Although these advantages they occupy a large space of 40 x 40 x 1.6 mm$^3$, 34.5 x 22 x 1.6 mm$^3$ and 47 x 47 x 0.675 mm$^3$ respectively. Another method for creating UWBs is to employ fractal geometries.

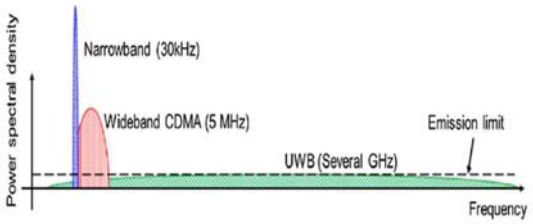


**Fig. 1.** Power spectral density versus frequency of the Narrowband, the Wideband, and the UWB [1].

The fractal structures have gained a lot of interest in the realization of UWB sensing antennas in miniaturized space. This type of antenna is known for its ability to create multiple resonant frequencies with their repetitive topology and ease installation in RF circuits. Various ultra-wideband antennas based on fractal geometry were introduced in the literature. The authors in [11] proposed a planar UWB antenna based on the fractal Sierpinski carpet to achieve a bandwidth of 9.6 GHz in a space of 24 x 30 x 0.8 mm$^3$. The hexagonal-shaped fractal antenna [12] and the Spanner Shaped fractal for

* Corresponding author: aichabembarka@gmail.com

cognitive radio antenna [13] have been also designed in the UWB range.

In this work, a flower-shaped fractal UWB antenna for Cognitive radio is presented and analyzed with two simulation tools CST Microwave Studio and verified using HFSS. The proposed geometry is planar and simply printed on the substrate's top layer, where the ground plane is partially below the substrate. From one ellipse considered fractal petal and two other ellipses scaled and rotated symmetrically to the petal, the flower shape of the antenna has been formed. The ellipses will be named also in this paper by "leaves". The antenna's most important characteristics are simulated to evaluate the performance of the proposed antenna. The antenna radiation efficiency is greater than 97 % and the peak realized gain attains 5.25 dBi. This paper is organized in this way; in section 1, we gave the geometry of the proposed fractal flower antenna. After section 1, we discuss the difference made in the reflection coefficient of the antenna radiated element with one leaf and with three leaves. The radiation efficiency, the realized gain, and also the radiation pattern is presented in this section. Finally, we conclude the work done.

## 2 Design of proposed antenna

The proposed antenna follows the principle of fractal geometry. The term "fractal" was introduced for the first time by the mathematician Benoit Mandelbrot in 1975, but it was discovered earlier by the mathematicians Pierre Fatou and Gaston Julia. The name "fractal" is derived from the Greek word "fractus," which means "broken" or "fractured." It is a structure made up of similar fragments of different sizes and orientations. The geometry and configuration of the proposed antenna are illustrated in Figure 2. It is constructed on Rogers RO4003C substrate ($\epsilon_r = 3.38$, $h = 0.81$, and δ=0.0027). The proposed antenna has a planar structure having a dimension of 12 x 16.9 mm$^2$. This antenna takes its shape from a flower, it was designed in accordance with the fractal concept in the interest of getting broad bandwidth. Herein, the flower patch is composed of three elliptical leaves. A central leaf (petal) surrounded by two similar leaves. The two leaves are scaled and rotated by $\boldsymbol{\theta}$=15° and $\boldsymbol{\theta}$=-15° in symmetry to the petal. The effective (electrical) semi-major axis of the central ellipse $a_{eff}$ takes into account stored energy in the fringing field of elliptical edge which can be calculated using equation (1):

$$a_{eff} = \frac{15}{\pi e (f_r)_{11}^{e,0}} \sqrt{\frac{q_{11}^{e,0}}{\varepsilon_r}} \quad (1)$$

e is eccentricity of elliptical patch.
$\varepsilon_r$ is permittivity of dielectric substrate.
$(f_r)_{11}^{e,0}$ is dual resonant frequency.
$q_{11}^{e,0}$ is called the Mathieu function, of the dominant $TM_{11}^{e,0}$ mode, which value can be obtained approximately from [14]:

$$q_{11}^{e} = -0.0049e + 3.7888e^2 - 0.7278e^3 + 2.314e^4 \quad (2)$$
$$q_{11}^{0} = -0.0049e + 3.8316e^2 - 1.1351e^3 + 5.2229e^4 \quad (3)$$

After the calculation of the effective semi-major axis, the physical semi-major axis a is derived from equation (4):

$$a_{eff} = a\left\{1 + \frac{2h}{\pi\varepsilon_r a}\left[\ln\left(\frac{a}{2h}\right) + (1.41\varepsilon_r + 1.77) + \frac{h}{a(0.286\varepsilon_r + 1.65)}\right]\right\}^{\frac{1}{2}} \quad (4)$$

Where h is the substrate height
Using the equation $b=a\sqrt{1-e^2}$ that connects the two semi-axes of an ellipse, we may determine the physical semi-minor axis b, then:

$$b_{eff} = b\left\{1 + \frac{2h}{\pi\varepsilon_r a}\left[ln\left(\frac{b}{2h}\right) + (1.41\varepsilon_r + 1.77) + \frac{h}{b}(0.286\varepsilon_r + 1.65)\right]\right\}^{\frac{1}{2}} \quad (5)$$

The major axis of the central leaf is **Lc**, as illustrated in Figure 2 and which is equal to 4.25 mm, while its minor axis length is **Wc**=1 mm. The scaled rotated leaves have a major axis length and a minor axis length **Le** and **We** respectively of 3.6 and 1.38 mm. The similar leaves helped to create more resonant frequencies at higher frequencies above 11 GHz and that is what fractal is known by. They are known by repeating shapes that give more resonant frequencies and these resonant frequencies can be controlled by changing the size of the repeated structures.

The ground plane is a critical part of antennas because it connects the distributed current to the power source ground. The proposed antenna ground plane is located at the other side of the substrate and to ensure that there is no electromagnetic field is kept between the radiated element and the ground plane as in [15]. A partial ground plane has been employed in this design. The proposed antenna ground is rectangular and its upper limit is far from the feed origin by 8 mm. Moreover, an inverted T-shaped slot truncated from its middle top edge helped to enhance the gain of the flower-shaped antenna in the band 11-16 GHz to higher values as can be shown in Figure 6. A microstrip feed line with 8.75 mm length provides a 50 Ω input impedance. Table 1 summarizes various dimensions of the proposed antenna geometry.

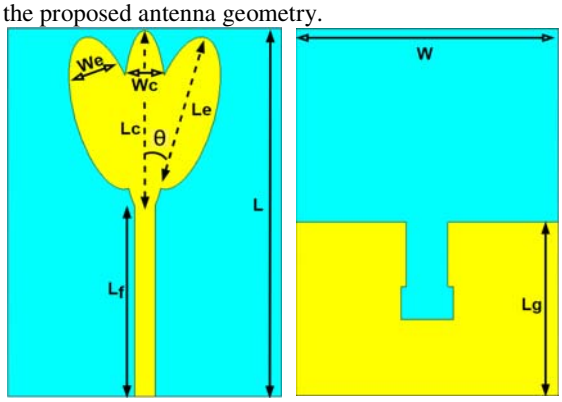


**Fig. 2.** Geometry of the proposed antenna (a) Top View (b) Botton View.

**Table 1.** Parameters of the fractal flower-shaped antenna.

| Dimension | Value(mm) | Dimension | Value(mm) |
|---|---|---|---|
| **L** | **16.9** | **W** | **12** |
| **Lg** | **8** | **Lf** | **8.75** |
| **Lc** | **4.25** | **Wc** | **1** |
| **Le** | **3.6** | **We** | **1.38** |
| $\boldsymbol{\theta}$ | **15** | | |

## 3 Results discussion

The results of the simulated reflection coefficient versus frequency are presented in Figure 3. A study has been done on the effect of the leaves on the reflection coefficient. Hence, we studied two cases; radiated element with only one ellipse and radiated element with three ellipses. The straight graph presents the reflection coefficient when a single elliptical patch is used, and the dotted curve provides the response of the radiated element with three ellipses. It can be clearly seen that the reflection coefficient increased when three ellipses were employed in comparison to one ellipse taking the -10 dB criteria. At first, the antenna was dual-band resonating at 9.62 GHz and 19.65 GHz. It can be clearly noticed that the reflection coefficient at the high band is a little high of -17 dB, which is not sufficient. On the other hand, after adding the two other leaves to the first leaf the antenna extended its resonant frequency from 7.36 to 19.57 GHz corresponding to nearly 49.64 % of the band added. Consequently, repeating the number of leaves proved that this technique helps to generate more resonant frequencies, then enhancing the antenna working band and improving its matching.

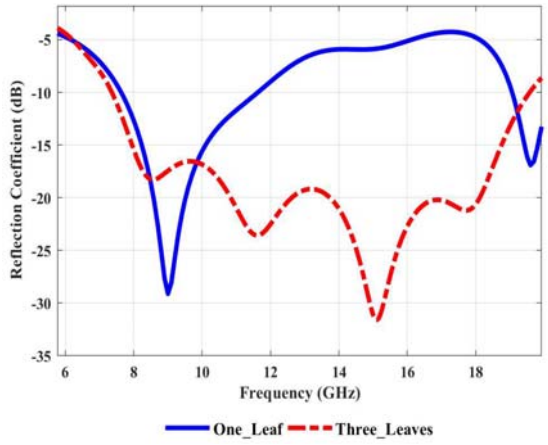


**Fig. 3.** Comparison of the simulated reflection coefficient between antenna with one ellipse and with three ellipses.

For further verification, we simulated the proposed structure with another software that uses a different calculating method which is HFSS. The design made in the 3D simulator CST was exported as a "Sat" file to the other 3D software (HFSS). The reflection coefficient in CST and HFSS of the proposed antenna is depicted in Figure 4. As can be seen that the response obtained from HFSS is almost the same reached previously in CST. The antenna has a minimum reflection coefficient of -31.59 dB at a frequency of 15.1 GHz. Moreover, the antenna is well matched all over the resonant band. Both responses proved that the proposed flower antenna exceeds the UWB spectrum. It has a relative bandwidth of 90.68 % (89.22 %) covering frequencies from 7.36 to 19.57 GHz (from 7.45 to 19.45 GHz) in CST and HFSS respectively.

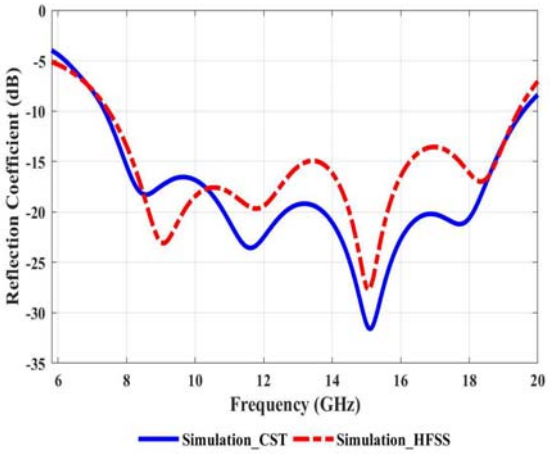


**Fig. 4.** Simulated reflection coefficient of the proposed antenna.

Two of the fundamental antenna parameters have been addressed in Figure 5, Figure 6, and Figure 7. The first one is the efficiency, also recognized as radiation efficiency, and the second one is realized gain. The last one is the radiation pattern.

The antenna efficiency $\boldsymbol{\varepsilon_R}$ is proportional to the power radiated from the antenna $\boldsymbol{P_R}$ and the power delivered to it $\boldsymbol{P_{in}}$, as shown in the below equation:

$$\boldsymbol{\varepsilon_R = \frac{P_R}{P_{in}}} \quad (6)$$

Figure 5 illustrates the simulated radiation efficiency of the proposed fractal antenna in comparison to the conventional partial ground plane. It can be observed that the partial ground plane with the inverted T-shaped slot improves the efficiency of the antenna. Herein, the lowest efficiency of the antenna is achieved at the frequency 19.57 GHz with 97.3 % when the ground has the T-shape truncation. On the other hand, a high amount of power is transmitted via the proposed antenna that is equal to 99.05 % as shown in simulation, which means there is only 0.95 % of the dissipated power. Our flower antenna has a high efficiency all over the working band from 7.36 to 19.57 GHz.

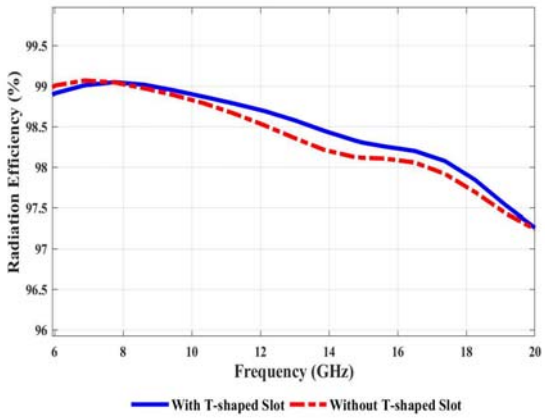


**Fig. 5.** Simulated radiation efficiency of the proposed flower-shaped antenna.

The simulated peak realized gain of the proposed antenna versus frequency is depicted in Figure 6. In the working band, the gain varies from 2.6 to 3.95 dBi for a maximum gain found with 4.147 dBi at the frequency of 12.2 GHz in CST. Whereas in HFSS it goes till 5.25 dBi at the frequency 19.45 GHz, and which varies from 2.67 to 5.25 dBi. Besides, the minimum value of gain is obtained at 15.6 GHz with 2.45 dBi. Making an inverted cut of a T-shape on the ground plane proved its potential to improve antenna gain for frequencies between 10 and 15 GHz. Hence, since the proposed antenna is compact and planar, the gain obtained is at an acceptable level.

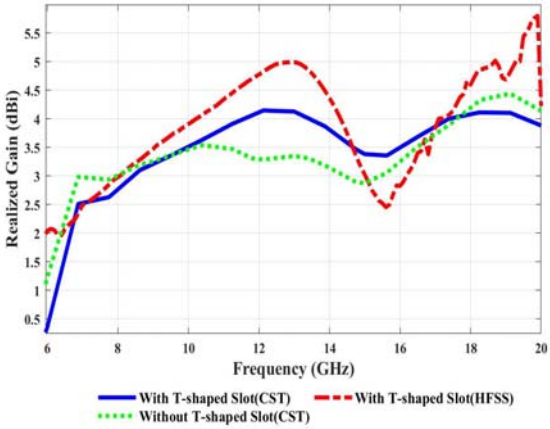


**Fig. 6.** Simulated realized gain of the proposed flower-shaped antenna.

For additional explanation of how the proposed antenna radiates energy out into the space and how it receives energy, the 3D and 2D view of the radiation pattern are presented in Figure 7. The calculations are performed at two frequencies 11.8 and 15 GHz to determine the antenna's stability behaviour in the operational band. According to simulations, the maximum obtained directivity of the antenna at the frequency 11.8 GHz is about 4.16 dBi, as demonstrated by the region covered in red color in Figure 7(a). At the other frequency (15 GHz), the flower antenna achieved a directivity of 3.46 dBi, as shown in Figure 7(b). The 2D pattern or also known as the polar plot of radiation pattern have been added in Figures (c)(d) in order to easily visualize the antenna radiation. It can be clearly observed that the antenna has an omnidirectional radiation in the E-plane (Co. Polarization) and in the H-plane (Cross. Polarization) it has bidirectional radiation. Figure 7(c) depicts the flower antenna polar plot at 11.8 GHz, the main lobe magnitude at this frequency is about 4.1 dB at the angle 342°, with angular 3-dB width of 57.7° for a cut done at phi component equal to 90°. Another polar plot of the antenna radiation pattern has been added in Figure 7(d) at 15 GHz. As shown in this Figure, a main lobe of magnitude 3.38 dB has been obtained at the direction 353°, while the angular 3-dB width is 54.1°.

Consequently, from the results obtained above the proposed antenna is compact and less dissipative, also it has a high gain and an omnidirectional radiation pattern stable among the working band, which makes the flower antenna very suitable for integration in UWB cognitive radio sensing applications.

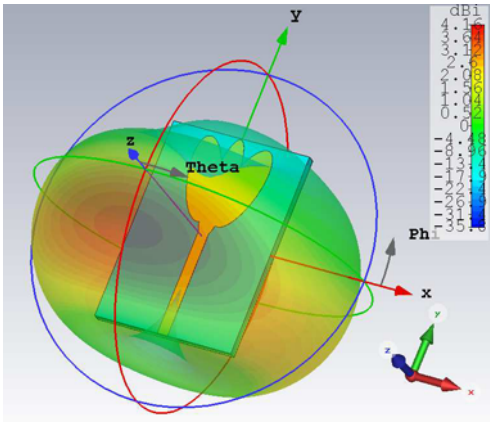


(a)

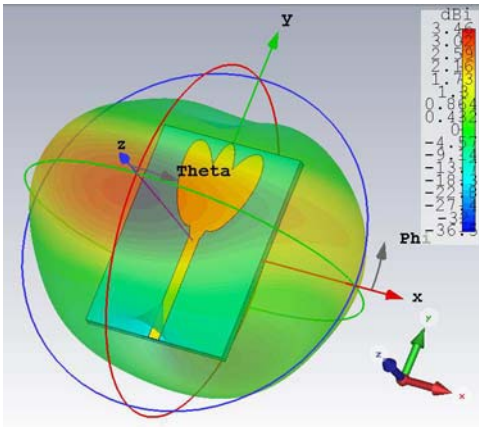


(b)

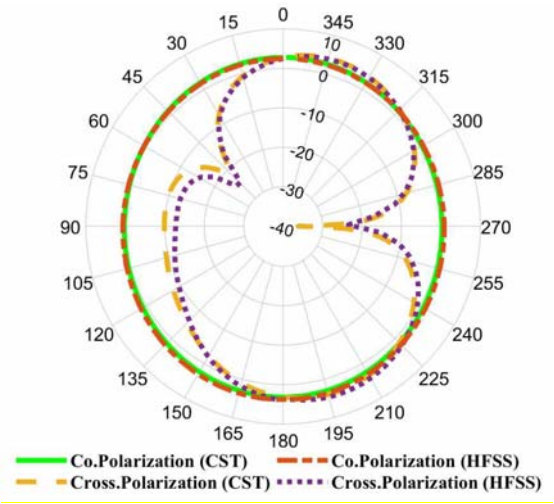


(c)

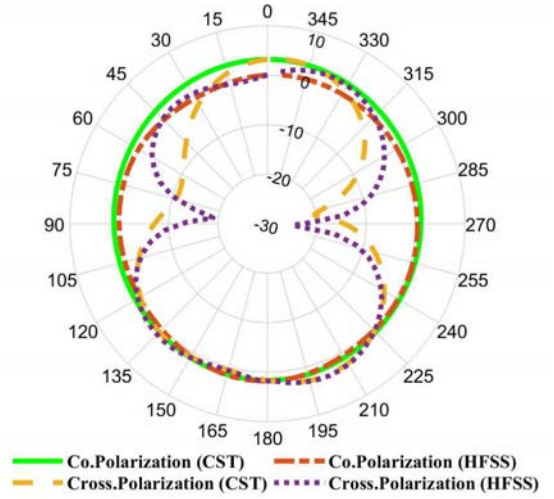


(d)

**Fig. 7.** Simulated radiation characteristics of proposed flower-shaped antenna (a) 3D at 11.8 GHz, (b) 3D at 15 GHz, (c) 2D at 11.8, (d) 2D at 15 GHz.

Table 2 summarizes a comprehensive comparison between the proposed antenna and previously published UWB antennas to determine the validity of the proposed design. As shown in the table, although the antenna in [18] has a high gain of 9.5 dBi, its dimension is vast, and its operating bandwidth is smaller than that of our structure. Even though the antenna in the literature [19] performs well, its size is quite large. In comparison to our antenna, we developed a miniaturized antenna in area of 12 x 16 x 0.81 $mm^3$ while maintaining a high efficiency ranging between 97.4 and 99.05 % and reasonable gain of 5.25 dBi and more than that it covers a wide bandwidth range of 90.68 %.

**Table 2.** Comparison between previously published UWB antennas and the proposed antenna.

| Parameter / Antenna | size [mm] | FR[a] [GHz]( FB[b] [%]) | Max. Gain[c] [dBi] | R. Eff.[d] [%] |
|---|---|---|---|---|
| **Proposed antenna** | **12x16.9 x0.81** | **7.36-19.57 (90.68)** | **5.25** | **> 97** |
| **[16]** | **25x38 x1.6** | **2.4-6 (86.71)** | **2.85** | **> 90** |
| **[17]** | **23x23** | **6.4-11.736 (58.7)** | **4.91** | **N/A** |
| **[18]** | **147x243 x 1.6** | **1.68-2.97 (55.5)** | **9.5** | **N/A** |
| **[19]** | **100x104 x0.5** | **2-9 (127.27)** | **6.5** | **> 98** |

[a]FR= Frequency Range. [b]FB=Fractional Bandwidth. [c]Max. Gain= Maximum Gain. [d]R. Eff= Radiation Efficiency.

## 4 Conclusion

A UWB antenna operating in a multi-band/multi-standard; the C X, Ku and K bands, of a fractal geometry were investigated in this paper. It has achieved a -10 dB relative bandwidth of about 90.68 % at the center frequency of 13.465 GHz. The fractal antenna was inspired by the shape of a flower that has three leaves which helped to obtain an ultra-wide bandwidth without increasing the substrate size. The overall size occupied by the antenna is 12 x 16.9 x 0.81 $mm^3$. The proposed antenna has good performances, it has high efficiency of 97 %, a good gain of 5.25 dBi at 19.45 GHz, and also it is well matched all over the operating band. Moreover, this flower antenna has an omnidirectional radiation pattern thus making it capable of spectrum sensing in cognitive radios. As future work, the research might be expanded to include the fabrication and testing of the design.

## References

1. N. Anveshkumar, A. S. Gandhi, and V. Dhasarathan, Cognitive radio paradigm and recent trends of antenna systems in the UWB 3.1–10.6 GHz, Wirel. Networks **26**, 3257–3274 (2020).
2. P. Palanisamy and M. Subramani, An integrated antenna for cognitive radio wireless sensor networks and HD video transmission applications, Int. J. RF Microw. Comput. Aided. Eng **31**, 11 (2021).
3. M. Y. Sandhu, S. Afridi, M. R. Anjum, B. S. Chowdhry, and Z. H. Khand, Ultra Wide Band (UWB) Horseshoe Antenna for Future Cognitive Radio Applications, Wirel. Pers. Commun **122**, 1087–1099 (2022).
4. M. Aggarwal and A. P. S. Pharwaha, Modified Koch curve broadband fractal antenna for spectrum sensing in cognitive radio, Int. J. Microw. Wirel. Technol **13**, 947–953 (2021).

5. M. Anouar and S. Larbi, *Array Antenna for Wireless Communication 5G*, In the Proceedings of the Third International Conference on Smart City Applications, SCA, 10-11 October 2018, Tetouan, Morocco (2018).
6. S. Guruswamy, R. Chinniah, and K. Thangavelu, A printed compact UWB Vivaldi antenna with hemi cylindrical slots and directors for microwave imaging applications, AEU - Int. J. Electron. Commun, **110** (2019).
7. Z. Zerrouk and S. Larbi, *Frequency Reconfigurable Antenna Using Infinity Complementary Split Ring Resonator for Wireless Communication*, in 2021 International Conference on Electrical, Computer and Energy Technologies, ICECET, 9-10 December 2021, Cape Town-South Africa (2021).
8. S. Heydari, K. Pedram, Z. Ahmed, and F. B. Zarrabi, Dual band monopole antenna based on metamaterial structure with narrowband and UWB resonances with reconfigurable quality, AEU - Int. J. Electron. Commun **81**, 92–98 (2017).
9. R. Sanyal, P. P. Sarkar, and S. Sarkar, Octagonal nut shaped monopole UWB antenna with sextuple band notched characteristics, AEU - Int. J. Electron. Commun, **110** (2019).
10. K. Sharma, A. Karmakarb, M. Sharma, A. Chauhan, S. Bansal, M. Hooda, S. Kumar, N. Gupta, A. K. Singh, Reconfigurable dual notch band antenna on Si-substrate integrated with RF MEMS SP4T switch for GPS, 3G, 4G, bluetooth, UWB and close range radar applications, AEU - Int. J. Electron. Commun **110**, 7–9 (2019).
11. R. Gurjar, D. K. Upadhyay, B. K. Kanaujia, and A. Kumar, A compact modified sierpinski carpet fractal UWB MIMO antenna with square-shaped funnel-like ground stub, AEU - Int. J. Electron. Commun, **117** (2020).
12. S. Tripathi, A. Mohan, and S. Yadav, Hexagonal fractal ultra-wideband antenna using Koch geometry with bandwidth enhancement, IET Microwaves Antennas Propag **8**, 1445–1450 (2014).
13. C. Waghmare and A. Kothari, *Spanner shaped ultra wideband patch antenna*, in 2014 Students Conference on Engineering and Systems, SCES, 28-30 May 2014, Allahabad, India (2014).
14. M. Gupta, K. K. Mutai, V. Mathur, and D. Bhatnagar, A Novel Elliptical Ring Microstrip Patch Antenna for Ultra-Wideband Applications, Wireless Pers Commun **114**, 3017-3029 (2020).
15. C. C. Lin, H. R. Chuang, and Y. C. Kan, A 3-12 GHz UWB planar triangular monopole antenna with ridged ground-plane, Prog. Electromagn. Res **83**, 307–321 (2008).
16. A. K. Gautam, A. Bisht, and B. K. Kanaujia, A wideband antenna with defected ground plane for WLAN/WiMAX applications, AEU - Int. J. Electron. Commun **70**, 354–358 (2016).
17. A. H. Majeed, A. S. Abdullah, K. H. Sayidmarie, R. A. Abd-Alhameed, F. Elmegri, and J. M. Noras, Balanced dual-segment cylindrical dielectric resonator antennas for ultra-wideband applications, IET Microw. Antennas Propag **9**, 1478–1486 (2015).
18. X. W. Dai, X. Y. Zhou, and G. Q. Luo, Wideband directional antenna system with different polarizations for wireless communication system, AEU - Int. J. Electron. Commun **75**, 119–123 (2017).
19. Z. Yang, H. Jingjian, W. weiwei, and Y. Naichang, An antipodal Vivaldi antenna with band-notched characteristics for ultra-wideband applications, AEU - Int. J. Electron. Commun **76**, 152–157 (2017).